

# Vibrational modes of hemoglobin in red blood cells

P. Martel,\* P. Calmettes,<sup>†</sup> and B. Hennion<sup>‡</sup>

\*Atomic Energy of Canada Limited, Research Company, Chalk River Nuclear Laboratories, Chalk River, Ontario, Canada K0J 1J0; and <sup>†</sup>Laboratoire Leon Brillouin (Laboratoire commun au Commissariat à l'Energie Atomique et au Centre National de Recherches Scientifiques), Centre d'Etudes Nucléaires de Saclay, 91191 Gif-sur-Yvette Cedex, France

**ABSTRACT** Equine red blood cells were washed in saline heavy water (<sup>2</sup>H<sub>2</sub>O) to exchange the hydrogen atoms of the non-hemoglobin components with deuterons. This led to novel neutron scattering measurements of protein vibrations within a cellular system and permitted a comparison with inelastic neutron scattering measurements on purified horse hemoglobin, either dry or wetted with <sup>2</sup>H<sub>2</sub>O. As a function of wavevector transfer **Q** and the frequency transfer  $\nu$  the neutron response typified by the dynamic structure factor  $S(\mathbf{Q}, \nu)$  was found to be similar for extracted and cellular hemoglobin at low and high temperatures. At 77 K, in the cells, a peak in  $S(\mathbf{Q}, \nu)$  due to the protein was found near 0.7 THz, approximately half the frequency of a strong peak in the aqueous medium. Measurements at higher temperatures (170 and 230 K) indicated similar small shifts downwards in the peak frequencies of both components. At 260 K the low frequency component became predominantly quasielastic, but a significant inelastic component could still be ascribed to the aqueous scattering. Near 295 K the frequency responses of both components were similar and centered near zero. When scattering due to water is taken into account it appears that the protein neutron response in, or out of, red blood cells is little affected by hydration in the low frequency regime where Van der Waals forces are thought to be effective.

## INTRODUCTION

There has been considerable interest recently in relating protein dynamics to biological activity (1). Various computer dynamics calculations (2–4) indicate that proteins may sustain large scale fluctuations on a picosecond timescale accessible to inelastic neutron scattering techniques. There have been several seminal papers describing how these techniques might be applied (5–9). Exactly how large scale fluctuations influence biological activity is not clear but presumably these fluctuations could be such that the static “lock and key mechanism” of biological activity (e.g., in enzyme-substrate interactions) would be modified to lower the free energy involved in specific contact interactions. For example, an enzyme about to engulf a substrate might be aided in its efforts by suitable modes of vibration that have motions related to a late stage of the encirclement process.

In a comprehensive paper outlining the theory of incoherent neutron scattering applicable to protein dynamics (8) it was pointed out that various regions of a protein molecule could be studied by selective deuteration. This would allow the density of vibrational states of the undeuterated portion to be projected out because of the high incoherent cross-section of the <sup>1</sup>H nuclei. We have applied this idea to red blood cells (RBC) which are known to have a rather special composition in that a large proportion (some 33%) of their mass is made up of hemoglobin (10). Another 60% or so of the red blood cell is aqueous and, on average, the remaining 7% is composed of membranes and other proteins in approxi-

mately equal proportions. In our experiments we have therefore sought to exchange the aqueous portions of the RBC so as to leave a large hemoglobin component which remains mainly hydrogenous.

It should be pointed out that neutron scattering is particularly suited for the present measurements because we wish to probe the dynamics of internal portions of the cell. This is so in part because of the possibility of isotopic substitution as noted above, and also because the neutron readily penetrates most condensed matter and this permits signal to be received from complex experimental environments. There have been many other neutron scattering measurements on proteins (9, 11, 12) that have examined bare protein in the presence of small percentages of deuterated water, and the success of these encouraged us to undertake the present experiment on a more complex system. To positively identify the protein component of the scattering we have also carried out measurements on purified hemoglobin, both dry and wetted with <sup>2</sup>H<sub>2</sub>O.

In this paper we first present the results of scattering (both elastic and inelastic) obtained from commercially available equine hemoglobin. This scattering was studied at 77 and 293 K. We then describe the scattering from equine RBC specimens in excess aqueous medium at 77, 170, 230, 260, and 295 K. The solvent scattering is also examined at these temperatures in separate measurements on the supernatant obtained after centrifugation of the specimens. Comparison of the scattering

from the cells and the supernatant then allows us to draw conclusions about the effects of an aqueous environment and of temperature on the protein dynamics. At temperatures near 77 K the dynamic structure factor  $S_a(Q, \nu)$  for the aqueous component shows a peak at a frequency  $\nu$  nearly double that of a peak due to the protein. These peaks have very little dependence on the wavevector transfer  $Q$  and the evolution of the scattering with increasing temperature is studied to see if there is evidence of any exchange of energy between the protein and its environment.

## METHODS

### Specimen preparation

For the first phase of the experiment horse hemoglobin was purchased from the Sigma Chemical Company (St. Louis, MO; catalogue number: H4632). In the experiments on dry hemoglobin measurements were made on this material as received. The wetted samples were prepared by simply adding 50 wt%  $^2\text{H}_2\text{O}$ . RBC samples were prepared from freshly drawn horse blood obtained from the Institut National de Recherche Agronomique (INRA) at Jouy-en-Josas near the reactor at Saclay. Upon extraction, 0.5% sodium citrate was added to inhibit coagulation. Sample preparation was begun some 5 h later and involved six precipitations of the RBC's with a Sigma Chemical Co. 2M centrifuge producing radial accelerations of 9,000 g for 15 min. After the first centrifugation the serum was removed by pipetting and the cells resuspended in the same volume of distilled water containing 9 g/l NaCl and a trace of ethylenediaminetetraacetic acid (EDTA). The latter procedure was repeated four more times but with  $^2\text{H}_2\text{O}$  instead of  $^1\text{H}_2\text{O}$ . In between centrifugations the samples were maintained at 4°C for periods of the order of 18 h to permit exchange of  $^1\text{H}$  by  $^2\text{H}$ . A final dilution involved addition to the solvent of 15 wt% deuterated dimethyl sulphoxide (DMSO). DMSO is a well-known cryoprotective agent (13) which prevents disruption of RBC's by ice. At every stage aliquots of the cells were removed and examined under an optical microscope. No evidence of damage was discerned. The final centrifugation preceded rapid cooling in a cryostat to a temperature of 77 K. The neutron response for two samples prepared in this manner was the same within experimental error.

To obtain the dry weight of the cells the samples were placed in test tubes capped by dialysis membranes and kept in a vacuum oven at 50°C for a minimum of 16 h.

### Neutron scattering

Most of the measurements employed the "constant- $Q$ " variable incident energy method of neutron scattering (14). This method utilizes a triple-axis spectrometer with fixed analyzer energy and an incident beam monitor whose sensitivity is directly proportional to neutron wavelength. With this procedure the raw data are directly proportional to the central quantity of interest in neutron scattering, which is the neutron response or the dynamic structure factor  $S(Q, \nu)$ . Thus, manipulation of the raw data is kept to a minimum so that a direct comparison of  $S(Q, \nu)$  data can easily be made. For any substance with a large fraction of hydrogen atoms, the generalized density of states  $G(\nu)$  can be extracted from  $S(Q, \nu)$  with certain approximations (9, 15). In this paper we shall only explore this latter aspect briefly because, as we shall show below, conversion to a  $G(\nu)$

representation tends to smooth out changes in the neutron response at low frequencies.

To increase sample volume while maintaining a high transmission the samples were contained in an annular chamber with inner and outer diameters of 3.0 and 3.2 cm, respectively. The cassette was constructed of vanadium. During the measurements its cylindrical axis was kept perpendicular to the scattering plane of the spectrometer to minimize angular effects. The data were normalized and corrected for background scattering by using measured transmissions along the radial centerline of the sample chamber. In all cases the transmission of the sample was  $> 80\%$ , and Monte Carlo calculations showed that the angular dependence of the multiple scattering was small. These calculations were in qualitative agreement with analytic theory (16) which indicates that for cylindrical symmetry, multiple scattering is a slowly varying function of  $\nu$  for "constant- $Q$ " measurements. The measurements on the purified hemoglobin samples were carried out using the C5 spectrometer at the NRU reactor (Chalk River, Ontario, Canada) and the RBC sample measurements were carried out on the 1T spectrometer at the Orphee reactor (Saclay, France). At frequencies below 1 THz the full width at half maximum (FWHM) of the gaussian instrumental resolution of the Chalk River measurements was 0.15 THz, and at Saclay, 0.20 THz. It may be noted that 1 THz =  $33.3 \text{ cm}^{-1} = 4.14 \text{ meV}$ .

## RESULTS

### Purified equine hemoglobin

Typical results on dry equine hemoglobin at 77 K are illustrated in Fig. 1. This figure shows an inelastic peak at  $\sim 0.8 \text{ THz}$  for all  $Q$ -values. Because these peaks in  $S(Q, \nu)$  arise from incoherent scattering processes there is no simple theory that accounts for their shape. However, they are a factor of approximately six wider than instrumental resolution and it is probable that they arise from many closely spaced vibrational modes of large amplitude. This is consistent with previous work on trypsin inhibitor and myoglobin (17) and molecular dynamics calculations on myoglobin (18). In the absence of a detailed calculations for hemoglobin, it has therefore been assumed that the collective nature of these modes can be described by a gaussian distribution.

Gaussian fits to these peaks indicate centroid values  $\nu_0$  of  $0.81 \pm 0.08$ ,  $0.91 \pm 0.12$ ,  $0.75 \pm 0.06$ , and  $0.81 \pm 0.10 \text{ THz}$  at  $Q$ -values of 1.0, 1.4, 1.85, and  $3.0 \text{ \AA}^{-1}$ , respectively. There is little evidence of a strong dependence of  $\nu_0$  on  $Q$ . For  $Q$ -values of 1.0, 1.4, and  $1.85 \text{ \AA}^{-1}$  the integrated intensity increases approximately as  $Q^2$  consistent with a harmonic response. The nearly vertical lines at the left of the plots represent fits to intense incoherent elastic scattering. This scattering was also fitted by gaussians and will be discussed later.

The results of similar measurements on dry hemoglobin at 293 K are depicted in Fig. 2. Here the inelastic scattering has shifted to much lower frequencies. The same gaussian analysis previously applied to the 77 K data yielded no significant finite frequencies within

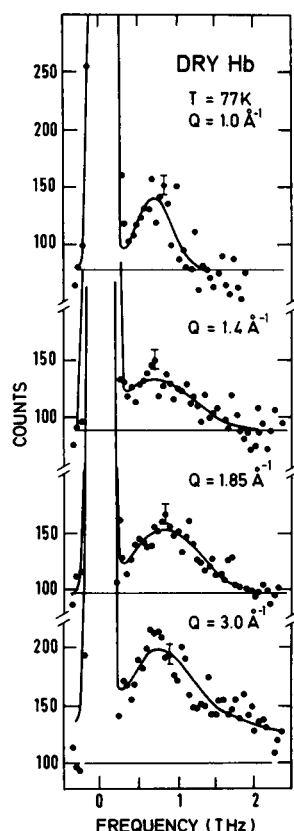


FIGURE 1 Neutron energy loss spectra of dry equine hemoglobin at  $T = 77$  K, and  $Q$  values of 1.0, 1.4, 1.85, 3.0  $\text{\AA}^{-1}$ . The lines represent gaussian fits (see text). As with all data presented in any given figure in the present paper, the same number of monitored neutrons was incident on the sample at all  $Q$  values.

experimental error for  $Q$ -values of 1.0, 1.4, 1.85, and 3.0  $\text{\AA}^{-1}$ . The shape of this scattering is similar to that seen for myoglobin at 300 K and suggests the presence of extra quasi-elastic scattering which may be accounted for by a damped oscillator model (17).

It should be noted that protein is known to be structurally sensitive to the presence of water. The use of dry lyophilized material might be criticized on the basis that partially hydrated proteins do not have full biological activity. One should note, however, that hemoglobin has a large percentage ( $\sim 80\%$ ) of its amino acids in alpha helices, which tend to be hydrophobic (19). Although the structure may be slightly distorted, we can therefore expect that a fair proportion of the amino acids in these alpha helices will be in a conformation similar to that of the fully hydrated protein. This interpretation is consistent with previous work (20–22) which indicates that as little as 0.2 g of water per 1 g of protein restores activity to dried enzymes.

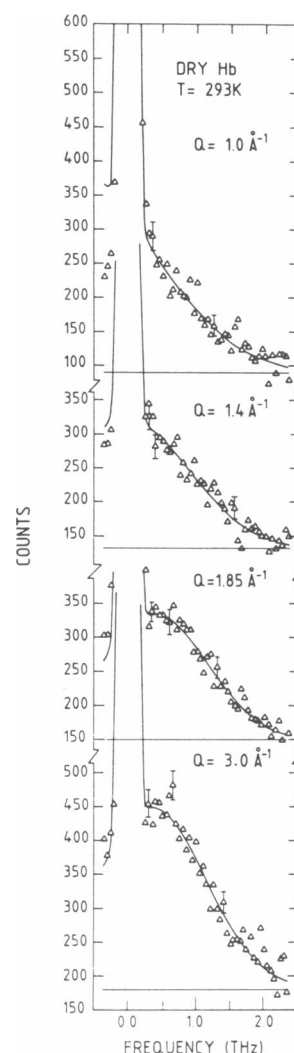


FIGURE 2 Neutron energy loss spectra of dry equine hemoglobin at  $T = 293$  K. Same sample as for Fig. 1.

In Fig. 3 we present results on a hemoglobin specimen containing 50 wt%  $^2\text{H}_2\text{O}$ . These results were obtained at 78 K and so they should be compared with those shown in Fig. 1. It may be noted that the wetted material also shows a peak at  $\sim 0.8$  THz. A gaussian fit indicated  $0.84 \pm 0.10$  as the centroid of the lower peak. There is also some evidence of a second peak which the fit indicates as having a centroid value of  $1.73 \pm 0.25$  THz. We shall show below that this second peak is due to the presence of water. The measurements on the hydrated sample were begun some 4 h after mixing and freezing. Thus there was time for a large proportion of the exchangeable protons in the native protein to be replaced by deuterons. Simultaneously, the aqueous component became "tagged" with hydrogen atoms having a

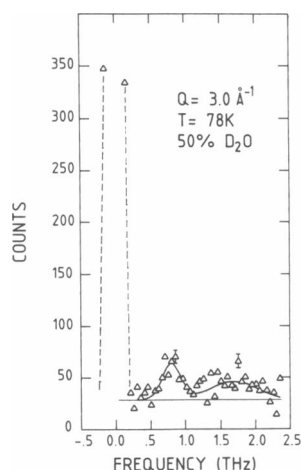


FIGURE 3 Neutron energy loss spectra of hemoglobin wetted by addition of 50 wt% heavy water ( $^2\text{H}_2\text{O}$ ). Note the indication of additional scattering at frequencies beyond 1.2 THz. The dashed (solid) lines represent gaussian fits to the elastic (inelastic) scattering.

large incoherent cross-section and this permitted observation of the peak in  $S(Q, \nu)$  which exists in ice. These measurements suggest that the presence of water does not significantly alter the low frequency response of the hemoglobin. It may be noted that the mean frequency of the peak due to the aqueous component is approximately double that due to the protein.

At room temperatures and above we might expect the frequencies of both the aqueous and protein components to fall drastically if only because, (a) water not associated with protein becomes liquid and (b) intimate contact with liquid water could lead to a damping of the vibrational modes in the protein. Recent molecular dynamics calculations (17) also suggest that frictional damping can account for an increased quasielastic component. Thus the room temperature results shown in Fig. 4 are not too surprising. These results illustrate measurements made on the same sample as in Fig. 3, but at 293 K. If these results are compared with those in Fig. 2 at the same  $Q$ -values, it is apparent that within experimental error the scattering is similar except possibly in a very low frequency region not easily accessible with the experimental resolution available in the present series of experiments. This low frequency region can be arbitrarily identified with the experimental points detached from the lower portions of the fits (solid lines) to the elastic scattering. These cannot be accounted for unless an additional gaussian is employed.

The occurrence of a strong elastic component provides additional information about the dynamics. The variation of this component as a function of  $Q$  allows us to extract an overall effective mean square atomic

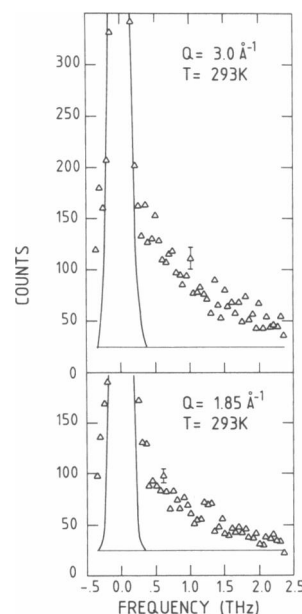


FIGURE 4 Neutron energy loss spectra of the sample as for Fig. 3, but at elevated temperature (293 K). Note that the inelastic scattering shows upward curvature as the frequency decreases toward the elastic peak delineated by our gaussian fitting procedure.

displacement  $\langle \Delta x^2 \rangle$ , by analyzing the integrated elastic peak intensities  $I(Q)$  centered on zero frequency with the equation

$$I(Q) = I(0) \exp(-\langle \Delta x^2 \rangle Q^2). \quad (1)$$

The results of the analysis are illustrated in Fig. 5 which displays values for the logarithm of  $I(Q)$  as a function of  $Q^2$  for dry hemoglobin. The straight lines through the data points represent the results of least squares fits and these yield values of:  $0.030 \pm 0.005$ ,  $0.039 \pm 0.002$ , and  $0.073 \pm 0.004 \text{ \AA}^2$  for  $\langle \Delta x^2 \rangle$ , at 5, 77, and 293 K, respectively. The hydrated sample yielded  $\langle \Delta x^2 \rangle = 0.045 \pm 0.004 \text{ \AA}^2$  at 77 K. The elastic scattering from the wetted hemoglobin was measured for only two  $Q$ -values at 293 K giving  $\langle \Delta x^2 \rangle \sim 0.093 \text{ \AA}^2$ . However, the latter value must be regarded with caution in view of recent results (12) which indicate that the  $Q^2$ -dependence of the logarithm of the elastic intensity of hydrated myoglobin is nonlinear at temperatures above 180 K. Molecular dynamics calculations for myoglobin (18) also suggest a nonlinear response which increases with increasing temperature. It is well known that the monomers of tetrameric hemoglobin have a structure similar to that of myoglobin. Neglecting contributions from exchanged hydrogen atoms in the deuterated solvent our limited measurements on the elastic components of the scattering suggest that the addition of  $^2\text{H}_2\text{O}$  tends to increase

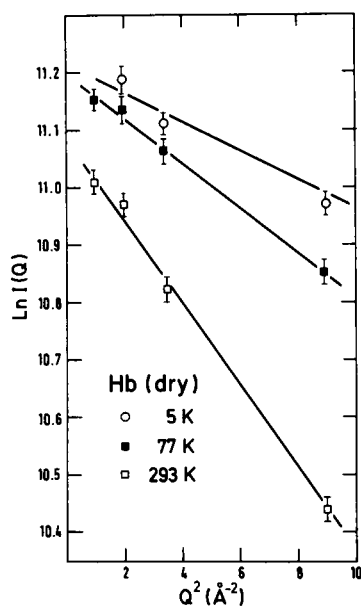


FIGURE 5 The natural logarithms of elastic peak intensities plotted vs.  $Q^2$  for hemoglobin at temperatures of 5, 77, and 293 K. The lines represent the results of fitting by the method of least squares.

the effective mean square atomic displacement of purified hemoglobin. This is in accord with other experiments (11) and with calculations (23) for purified protein in the presence of small percentages of water.

### Equine hemoglobin in red blood cells

The nature of our scattering measurements on intracellular hemoglobin is best understood by considering the raw data presented in Fig. 6. The measurements illustrated here were made with the specimen at 77 K. Note a break in the data at low frequencies because the elastic scattering near zero frequency has been divided by a factor of 20 to bring it on scale. The full width at half maximum of the plastic peaks is 0.21 THz, essentially the width of the spectrometer resolution function. In the inelastic region the uppermost curve represents the total scattering comprised of cells plus solvent. Two features are evident here. There is a strong peak at  $\sim 1.5$  THz and a shoulder which appears near 0.8 THz. The two next lower data sets (denoted by squares and crosses) indicate that a large fraction of the scattering comes from the frozen aqueous component. The squares represent measurements on the supernatant and the crosses represent measurements on the aqueous solvent used in the last dilution but with 10 wt%  $^1\text{H}_2\text{O}$  present. This  $^1\text{H}_2\text{O}$  serves to magnify the response in  $S(Q, \nu)$  of the translational modes of the water molecules in ice. The nature of these modes and a review of pertinent neutron

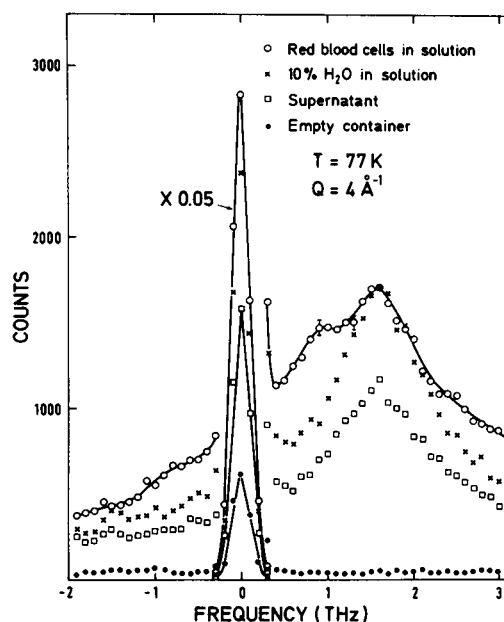


FIGURE 6 Raw neutron scattering results from red blood cells in frozen solution (circles), fresh solvent containing 10% light water (crosses), separated solvent (squares), and empty vanadium container (dots). All spectra obtained with the same number of neutrons incident on the sample, and at  $T = 77$  K. Neutron energy gain values of  $S(Q, \nu)$  appear at negative frequency values (see text). By comparison with the aqueous and supernatant spectra, additional intensity can be seen in the red blood cell (RBC) data at frequencies below 1.0 THz.

spectra has been discussed by Tse et al. (24). The presence of ordinary hexagonal ice was deduced from Bragg peaks that indicated the presence of such ice (25) at temperatures of 260 K or lower, in all samples. By comparing the data represented by the crosses and squares we conclude that the aqueous component in our cellular specimens were deuterated to better than 90%. In what follows we shall show data obtained by subtracting the supernatant scattering from the total scattering. Even without corrections for absorption, it can be seen from Fig. 6 that such a subtraction will lead to excess intensity in the frequency region close to 0.8 THz. This excess is to be ascribed to hemoglobin in the red blood cells. Note that additional evidence for excess intensity can be seen in the neutron energy gain part of the upper curve at negative frequency transfer where a "bump" appears at  $\sim -0.8$  THz. The large peak at 1.5 THz is suppressed at negative frequency transfer, because the Boltzman factor (detailed balance) diminishes the response very much for large negative values of  $\nu$ .

To properly interpret the total scattering it is instructive to first consider the nature of the supernatant component which has had its cross-section enhanced by residual hydrogens left over from incomplete exchange.

Results for  $Q = 3.0 \text{ \AA}^{-1}$  are depicted in Fig. 7. The central peak plotted with intensities divided by a factor of 20 represents the elastic scattering at 77 K. For temperatures of 260 K or lower, it is apparent that  $S(Q, \nu)$  exhibits a peak at  $\sim 1.5 \text{ THz}$ . At 295 K, however, the scattering has the monotonic variation depicted by the dashed line. It may be noted that as the temperature increases from 77 to 260 K, there is a slight shift in peak frequency to lower values, but the main change is a "filling in" of the minimum between the elastic and inelastic peaks. Thus, somewhere between 260 and 295 K (probably 273 K) the peak in  $S(Q, \nu)$  disappears. The general shape of  $S(Q, \nu)$  for the supernatant seems to have little  $Q$  dependence. For  $Q = 1.85$  (Fig. 8) the elastic scattering intensity is higher and the inelastic lower than for the corresponding regions in Fig. 7, but the form is the same. This is explicable in terms of the Zemach-Glauber formalism for incoherent scattering (8). As before there is a progressive increase in quasielastic intensity between the elastic and inelastic regions as the temperature increases. The same features were also observed for  $Q$  values of 1.4 and  $4.0 \text{ \AA}^{-1}$ .

When these supernatant components are subtracted from the total scattering, the resulting  $S(Q, \nu)$  should be dominated by the hemoglobin in the RBC specimens. The resulting  $S(Q, \nu)$  will be referred to as  $S_p(Q, \nu)$ . To obtain  $S_p(Q, \nu)$  a point-by-point subtraction was carried

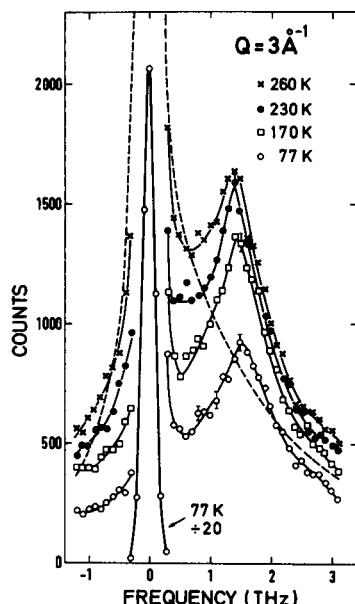


FIGURE 7 Neutron spectra from the separated solvent (supernatant) observed at various temperatures and at  $Q = 3.0 \text{ \AA}^{-1}$ . Note the existence of a peak in  $S(Q, \nu)$  near 1.5 THz, for  $T = 260 \text{ K}$  or less. The dashed line represents results (data points omitted for clarity) obtained on the supernatant in the liquid state.

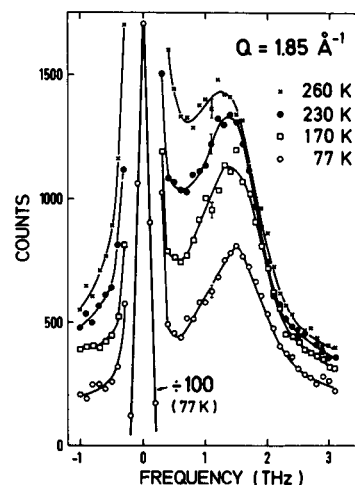


FIGURE 8 Results similar to those illustrated in Fig. 7, but for  $Q = 1.85 \text{ \AA}^{-1}$ . Note the similarity of the scattering in Figs. 7 and 8.

out and typical results are shown in Fig. 9 for  $Q = 3.0 \text{ \AA}^{-1}$ . The subtraction procedure took account of the absorption of the various components of the system and the dry weight of the cells (25% of the total specimen weight) determined after dehydration in a vacuum oven. Uncertainties such as those due to the presence of a small fraction of membrane and extraneous proteins remain, but tests with changes in the dry weight value by 5% indicated that the general shape of the net scattering curves remained similar. Some of the curves in Fig. 9 show a hint (e.g., the 77 K data) of the supernatant peak at  $\sim 1.5 \text{ THz}$ , but such a remnant is not unexpected because a certain amount of water, perhaps as much as 4 wt%, is strongly bound to any protein sample that retains its functional structure. Thus  $S_p(Q, \nu)$  can contain contributions from strongly bound water, especially in a natural environment. Another potential contribution to additional intensity at  $\sim 1.5 \text{ THz}$  is suggested by molecular dynamics calculations (17, 18) which indicate the possible existence of a second peak intrinsic to myoglobin at about twice the frequency of the lower protein peak.

The lines through the data points represent fits involving three gaussians and a frequency-dependent inelastic background (FDIB) determined by the spectrometer resolution function. The FDIB is frequency dependent for a triple-axis spectrometer because the resolution function broadens as the frequency increases. Three gaussians were invoked to account for peaks due to: (a) elastic scattering, (b) scattering by protein near 0.8 THz, (c) scattering due to water of hydration (and possibly protein) centered near 1.5 THz. Detailed balance (15) was taken into account in the fitting. The

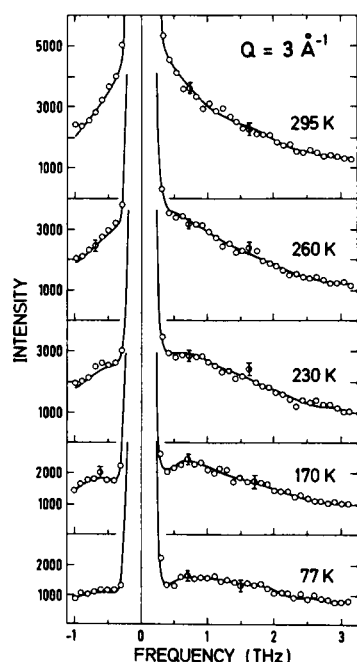


FIGURE 9 Net neutron scattering response for red blood cells after subtraction of the solvent component (see text). A remnant of the solvent scattering can be seen in some of the spectra and this is thought to arise at least in part from bound water. As the temperature increases the intensity minimum near 0.5 THz becomes less marked. The lines represent a fit with three Gaussians and a frequency-dependent background calculated as a function of spectrometer resolution. Detailed balance was included in the fitting. All spectra are for  $Q = 3.0 \text{ \AA}^{-1}$ . Numerical values for the hemoglobin component are listed in Table 1. At 295 K, the fit for the hemoglobin component yielded an ill-defined centroid frequency of  $0.10 \pm 1.50 \text{ THz}$ .

positions, widths, and intensities of all three Gaussians were allowed to vary freely. The instrumental resolution was taken into account during the Gaussian fitting procedure. It can be seen that the fitted lines describe the data quite well. At 77 and 170 K the existence of a broad inelastic spectrum can be readily discerned; its maximum is  $\sim 0.7\text{--}0.9 \text{ THz}$ . At 170 K, the inelastic scattering region is still separate from the elastic region by a minimum, but at 260 K the two tend to merge into one another. At 295 K, there is no longer a region that can be uniquely ascribed to the protein by our fitting procedure. Fitted values for the low-frequency protein component at  $Q = 3.0 \text{ \AA}^{-1}$  can be found in Table 1. The increases in intensity as the temperature increased were in agreement with increases due to Bose-Einstein statistics. This was true within experimental error for both inelastic components (protein and "aqueous") of the scattering at, or below, 260 K.

The same general neutron response was also obtained at other  $Q$  values. This can be seen by comparing the

TABLE 1 Results of Gaussian analysis of RBC hemoglobin components

$Q$	$T$	$\nu_0$	FWHM
$\text{\AA}^{-1}$	$K$	$\text{THz}$	$\text{THz}$
1.4	230	$0.49 \pm 0.09$	$0.58 \pm 0.27$
1.4	260	$0.12 \pm 0.03$	$1.58 \pm 0.16$
1.85	77	$0.64 \pm 0.06$	$0.78 \pm 0.09$
1.85	170	$0.54 \pm 0.06$	$0.61 \pm 0.04$
1.85	230	$0.52 \pm 0.07$	$0.91 \pm 0.10$
1.85	260	$0.21 \pm 0.07$	$1.79 \pm 0.18$
3.0	77	$0.61 \pm 0.12$	$0.79 \pm 0.16$
3.0	170	$0.58 \pm 0.06$	$0.85 \pm 0.10$
3.0	230	$0.46 \pm 0.10$	$0.96 \pm 0.17$
3.0	260	$0.15 \pm 0.06$	$1.59 \pm 0.60$
4.0	77	$0.65 \pm 0.07$	$0.69 \pm 0.07$
4.0	170	$0.52 \pm 0.06$	$0.72 \pm 0.16$
4.0	230	$0.46 \pm 0.09$	$0.85 \pm 0.07$
4.0	260	$0.12 \pm 0.04$	$1.60 \pm 2.06$

The central frequencies and full widths at half maximum are denoted by " $\nu_0$ " and "FWHM," respectively.

data points in Fig. 10 with those in Fig. 9. The fitting procedure accounts for experimental frequency response quite well at all temperatures and  $Q$  values. However, there is a slight systematic underestimate by the model at "negative" frequencies because higher order beam contamination becomes increasingly large in this frequency region.

It appears that, near 230 K, the protein dynamics are in a temperature range where changes can occur. It has

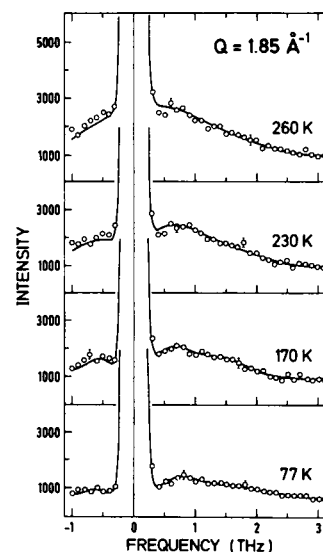


FIGURE 10 Net neutron response for  $Q = 1.85 \text{ \AA}^{-1}$  of equine red blood cells after subtraction of the solvent component as outlined in the text. This figure may be compared with Fig. 9 to verify that there is little frequency dependence on  $Q$ .

recently been shown that above 180 K the dynamical response in myoglobin changes considerably (12) and there is the suggestion of a coupling of fast local motions to slower collective motions, "which is a characteristic feature of other glass forming systems." It may be that collective motions are hindered in the cells due to freezing of the aqueous matrix below 230 K; nearby ice could restrict motion at the protein surface.

An examination of Figs. 9 and 19 indicates that the neutron frequency response is virtually independent of  $Q$  in the  $Q$  range of these measurements. To enhance statistics we have summed the data for three  $Q$  values (1.85, 3.0, and 4.0  $\text{\AA}^{-1}$ ). Plots of the resulting summed data are shown in Fig. 11. The solid lines represent fits using the model described above. Taken as a whole, the data in the figure support the contention that a change in the protein dynamics occurs somewhere in the range  $230 < T < 260$  K. The mean square displacement of iron and some of the amino acids of myoglobin is known (26) to change abruptly as a function of temperature as 200 K is approached. A transition at 180 K in the low frequency dynamics of myoglobin has been deduced from recent neutron scattering measurements (12). These differences may simply reflect different methods of interpretation as well as the fact that different molecules are involved.

A summary of the intracellular hemoglobin response appears in Table 1, for various  $Q$  values and tempera-

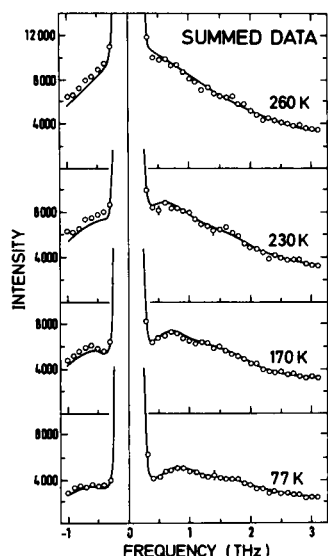


FIGURE 11 Summed data for measurements carried out at the three  $Q$  values, 1.85, 3.0, and 4.0  $\text{\AA}^{-1}$ . The lines result from the same fitting procedure defined earlier. The statistical errors are little greater than the size of the data points. As the temperature increases the lowest peak ascribed to the hemoglobin merges with the elastic scattering.

tures. As the temperature,  $T$ , increases the centroid of the frequency is seen to decrease from  $\sim 0.65$  THz at 77 K, to  $\sim 0.15$  THz at 260 K. Although the widths are similar, the intracellular centroid frequencies seem to be slightly lower than those for the extracted and purified hemoglobin, but the statistical accuracy of the data for the latter is not sufficient to render the difference definitive. There is a tendency for the widths to increase as  $T$  increases, especially as  $T = 260$  K is approached. During the fitting, the frequency of the "aqueous" component was allowed to vary freely, but except for  $T = 295$  K, it always ended up near 1.4 THz within statistical error. For temperatures below 295 K, the widths of the elastic peaks remained constant within experimental error. At 295 K the elastic peak was broader by  $\sim 30\%$  than at lower temperatures. As noted above, the intensities of both inelastic components was in accord with Bose-Einstein statistics at all four temperatures. The summed data yielded centroid values for the lower peak of:  $0.62 \pm 0.03$ ,  $0.54 \pm 0.03$ ,  $0.48 \pm 0.09$ , and  $0.08 \pm 0.09$  THz at  $T = 77, 170, 230$ , and 260 K, respectively. The corresponding values for full widths at half minimum (FWHM) were:  $0.73 \pm 0.07$ ,  $0.70 \pm 0.20$ ,  $0.92 \pm 0.26$ , and  $1.63 \pm 0.06$  THz. At 77 K, the equivalent FWHM of the dry protein was  $0.9 \pm 0.1$  THz.

A graphical summary of the results of the fits to the protein data from the RBC measurements is presented in Fig. 12. It can be seen that the fits for various  $Q$  values all suggest a strong temperature dependence of  $S_p(Q, \nu)$  between 230 and 260 K. The variations in width and frequency are in accord with those found from an analysis of summed data. The lines through the data points are merely guides to the eye but they suggest strongly that the centroid frequencies  $\nu_0$  go to zero near the melting point of ice. It was also found that the quality of the fits to the data at 230 K was rather variable; this may be a further indication that the system was near a transitional temperature region.

It can be shown (8, 15) that a generalized density of states  $G(\nu)$  can be obtained from the incoherent scattering response by evaluating:

$$G(\nu) = AB(\nu)C(0, \nu), \quad (2)$$

where  $A$  is a constant,  $B(\nu) = \nu(e^{h\nu/KT} - 1)$  and  $C(0, \nu) = \lim_{Q \rightarrow 0} S(Q, \nu)/Q^2$ .

As usual the Planck and Boltzman constants are denoted by  $h$  and  $K$ . Eq. 2 is an approximation valid under certain conditions (8). As indicated above, we have chosen to compare most of our measurements of the incoherent structure factor  $S(Q, \nu)$ , directly. Nevertheless, for completeness we now consider briefly a conversion of the neutron response data for  $T = 170$  K



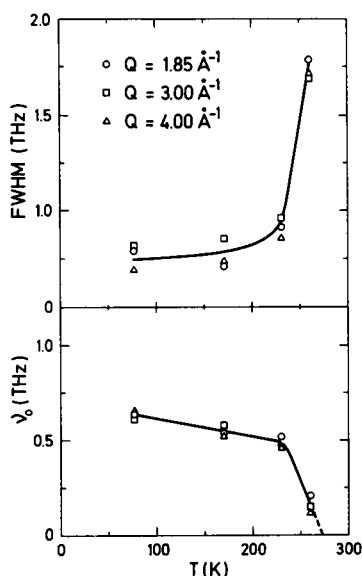


FIGURE 12 Graphical summary of selected data from Table 1 illustrating the temperature dependence of the peak due to the low-frequency protein component of the scattering from red blood cells. The lines through the data are merely guides to the eye. Note the change in both peak width and frequency at temperatures  $> 230$  K.

to a  $G(\nu)$  form. To obtain the limiting value indicated for  $C(0, \nu)$ ,  $\ln [S(Q, \nu)/Q^2]$  was plotted for various values of  $Q^2$  and the  $Q = 0$  value of the logarithm found by linear extrapolation. Values of the antilogarithm,  $C(0, \nu)$ , are shown in Fig. 13. The small scale undulations in the curve are not statistically significant, but were retained for purposes of illustrations. It may be noted that  $C(0, \nu)$  is very similar in form to the summed data for  $T = 170$  K shown in Fig. 11. This is not unexpected in view of the lack of dispersion evident from a comparison of the spectra in Figs. 9 and 10.

The variation of  $B(\nu)$  is also shown in Fig. 13. It can be seen from the figure that multiplication of  $C(0, \nu)$  by  $B(\nu)$  will tend to diminish any relief in the variation of the former function as  $\nu$  approaches zero. Thus Eq. 2 does not serve as a sensitive test for comparison with calculations of low frequency modal distributions. This can readily be seen in the figure, for example, where features in the  $A, B$  region of  $C(0, \nu)$  are barely reflected in  $G(\nu)$ . On the other hand  $B(\nu)$  tends to amplify little details such as  $C$ , at higher frequency values of  $G(\nu)$ . As a result the dip at  $C$  produces the prominent feature  $C'$ , in  $G(\nu)$ . It seems that for comparison with our data it may be necessary to undertake normal mode calculations since the eigenfrequencies and eigenvectors thereby obtained could be used to calculate  $S_p(Q, \nu)$  directly. Even then, however, anharmonic effects would have to

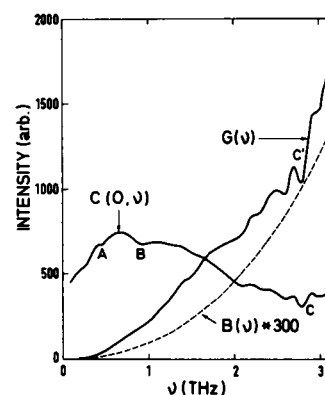


FIGURE 13 Conversion of  $T = 170$  K data to a generalized density of states,  $G(\nu)$ . The solid line ABC represents the extrapolated values,  $C(0, \nu)$ , of  $S(Q, \nu)/Q^2$  extrapolated to  $Q = 0$ . The dashed line represents values of 300 times the thermal factor,  $B(\nu)$ , which multiplies  $C(0, \nu)$  to obtain  $G(\nu)$ . It can be seen that features like  $AB$  are diminished at low frequencies, while small features like  $C$  are magnified (to become  $C'$ ) at higher frequencies. Hence neutron scattering results at low frequencies are best compared directly in terms of  $S(Q, \nu)$ .

be taken into account, possibly by doing molecular dynamics calculations in parallel. Recent calculations (18) indicate an advanced method for the direct evaluation in time " $t$ " of the intermediate neutron scattering function  $I(Q, t)$  from the atomic trajectories found by molecular dynamics,  $S(Q, \nu)$  is then calculated by numerical Fourier transformation of  $I(Q, t)$ .

It should perhaps be noted that although  $S(Q, \nu)$  presents the best test for calculations, the evaluation of  $G(\nu)$  is very important. Even though  $G(\nu)$  may appear to be relatively featureless, it is a function of considerable biological importance, as it determines the dynamic contribution to the thermodynamics of the system. Also, any deviations can be used for comparisons with simple models (e.g., fracton, Debye, etc.).

The variation of logarithmic values for the integrated intensities of elastic scattering from intracellular protein was found to be nonlinear as a function of  $Q^2$ , for temperatures of 170 K, or higher. An upward curvature similar to that previously seen in  $^2\text{H}_2\text{O}$  wetted myoglobin at temperatures above 202 K (12) was observed. A linear fit for  $T = 77$  K yielded  $\langle \Delta x^2 \rangle = 0.014 \pm 0.003 \text{ \AA}^2$ . This is considerably less than the value  $(0.039 \pm 0.002 \text{ \AA}^2)$  reported above for dry hemoglobin. As noted above the presence of 50 wt % water in the purified protein samples increased  $\langle \Delta x^2 \rangle$  to  $0.045 \pm 0.004 \text{ \AA}^2$  at 77 K. The supernatant itself gave  $\langle \Delta x^2 \rangle = 0.059 \pm 0.004$ . Our unexpectedly low value for cellular hemoglobin is clearly a topic for further investigation, but is outside the scope of the present study.

## DISCUSSION

Before discussing the low frequency response it is perhaps worth commenting on a few characteristics of the overall effective mean square displacements,  $\langle \Delta x^2 \rangle$ , determined with Eq. 1. As noted by Smith et al. (18) incoherent elastic neutron measurements have the virtue that they do not contain a static disorder contribution (26). Although no temperature-dependent measurements have been reported for hemoglobin, it is instructive to compare our results with molecular dynamics (MD) calculations and measurements on other proteins. At 80 K, Hartmann et al. (26) found a  $\langle \Delta x^2 \rangle$  value of  $0.063 \text{ \AA}^2$  for crystallized myoglobin; they estimated that this value contained a disorder component of  $\sim 0.025 \text{ \AA}^2$ . Their net dynamical component therefore compares favorably with either of our values of  $0.039$  and  $0.045 \text{ \AA}^2$  for dry and wet hemoglobin, respectively, at 77 K. The increase in  $\langle \Delta x^2 \rangle$  due to solvation is of the same order ( $\sim 15\%$ ) as that suggested by MD calculations (23) for lysozyme. At room temperature our  $\langle \Delta x^2 \rangle$  value for dry hemoglobin ( $0.073 \text{ \AA}^2$ ) seems small compared with calculations (18) and measurements which place the dynamical component of  $\langle \Delta x^2 \rangle$  for myoglobin in excess of  $0.13 \text{ \AA}^2$ . However, our measurements at 293 K suggest a 27% increase in  $\langle \Delta x^2 \rangle$  on solvation, in rough agreement with MD calculations (23) for lysozyme. Our value of  $\langle \Delta x^2 \rangle$  for hemoglobin in red blood cells at 77 K, seems low at  $0.014 \pm 0.003 \text{ \AA}^2$  when compared with MD calculations (18) for myoglobin; these calculations indicate that for a myoglobin molecule, trapped in conformational space for times greater than 100 ps, an average mean square fluctuation of  $0.025 \pm 0.014 \text{ \AA}^2$  occurs at 80 K.

A significant result of the present measurements is the similarity of the low frequency neutron scattering response for wet and dry hemoglobin in and out of a cellular environment. Other measurements on myoglobin yield similar results. The possibility that different proteins would have similar vibrational spectra at low frequencies was indicated some time ago by normal mode calculations (27) which showed a peak in the density of states distribution for proteins as disparate as bovine pancreatic trypsin inhibitor, crambin, ribonuclease, and lysozyme. Although these density of states distributions showed some differences in detail, the presence of a peak in the 1 THz region was common to all. Our  $S_p(\mathbf{Q}, \nu)$  results are also compatible with the existence of a peak at low temperatures, but at room temperatures there appears to be a large downward shift in frequency apparently independent in large part to the presence of water. The normal mode calculations did not take account of solvent effects. It may also be noted

that normal mode calculations cannot explicitly take account of anharmonic effects, and it might therefore be concluded that such calculations are strictly applicable to proteins at low temperatures. The atomic motions in protein are liable to be somewhat anharmonic at room temperatures. More recent molecular dynamics calculations (18) for myoglobin in vacuo indicate that a peak near 0.7 THz becomes much less distinct at room temperatures where it tends to merge with an enhanced quasielastic component at lower frequencies.

Another significant result concerns the detailed temperature dependence of the different components of the inelastic scattering. Below 230 K the temperature dependence of the centroid frequencies is slight for both the protein and aqueous components. According to Brooks and Karplus (23) the strength of any solvent-protein interaction requires that the timescale of the solvent motions overlaps that of the protein and also the protein atoms must be coupled spatially to the solvent atoms. However, in red blood cells, our simplified analysis revealed no significant changes in position or width of the "aqueous" peak, concomitant with the downward shift in the centroid of the protein component at 260 K. Thus there was no conclusive evidence of resonant energy exchange between the solvent and the protein. From Figs. 7 and 8 it can be seen that although the peak in the supernatant response did not shift appreciably, there was a considerable enhancement in the intensity in the dip between the elastic and inelastic peaks when  $T$  increased. Indeed on going to room temperature there is no dip remaining and the scattering then seems to be largely quasielastic. This could account for some of the difference between the spectra for dry and wet hemoglobin in the low frequency regime ( $\nu < 0.5 \text{ THz}$ ).

It has long been known (28) that hemoglobin molecules in erythrocytes are closely packed and exhibit short-range order typical of a close-packed lattice. However, they are not so tightly packed that they do not rotate. Thus hemoglobin molecules in cells seem to cluster and it may be that their distribution is different from that of pure hemoglobin in solution. Such a difference in distribution (if it exists) does not seem to strongly modify the vibrational response observed in the present measurements.

The existence of a low-lying peak near 0.8 THz has been observed in the Raman spectra of many globular proteins (29, 30). The ubiquitous nature of these low-lying modes suggests that they arise from nonspecific forces such as Van der Waals interactions between neighboring amino acids. It may be noted that these forces have been included in calculations (3, 27, 31) which indicate correlated atomic displacements at these low frequencies. An interesting experimental result on

myoglobin (32) could be germane to the present observations on hemoglobin. Mossbauer measurements of the recoilless fraction on  $^{57}\text{Fe}$ -enriched oxy- and carbon monoxy-myoglobin in frozen aqueous solution indicated that the temperature dependence of  $\langle \Delta x^2 \rangle$  for Fe could be interpreted quite well up to 180 K assuming an intrinsic phonon frequency of 0.75 THz. Note that our observations indicated negligible shifts in phonon frequencies of hemoglobin up to  $T = 230$  K.

We acknowledge expert technical advice from Dr. B. Fleur of Laboratoires Bruneau, Boulogne-Billancourt in connection with cryoprotection of the RBC samples. Thanks are also due to Dr. J.-M. Babilliot of l'Institut National de Recherche Agonomique, Jouy-en-Josas, for the gift of fresh samples of equine blood. We are indebted to Dr. Jeremy Smith for helpful discussions and a critical reading of the manuscript. One of us (Dr. Martel) wishes to thank the Laboratoire Leon Brillouin for kind hospitality and encouragement during a sabbatical year spent at the laboratory.

Received for publication 3 April 1990 and in final form 6 September 1990.

## REFERENCES

- Weiss, M. A., D. T. Nguyen, I. Khait, K. Inouye, B. H. Frank, M. Beckage, E. O'Shea, S. E. Shoelson, M. Karplus, and L. J. Neuringer. 1989. Two-dimensional NMR and photo-CIDNP studies of the insulin monomer: assignment of aromatic resonances and applications to protein folding, structure and dynamics. *Biochemistry*. 28:9855-9873.
- Swaminathan, S., T. Ichiye, W. F. van Gunsteren, and M. Karplus. 1982. Time dependence of atomic fluctuations in proteins. *Biochemistry*. 21:5230-5241.
- McCammon, J. A., and S. C. Harvey. 1988. Dynamics of proteins and nucleic acids. Cambridge Univ. Press, Cambridge, U.K.
- Brooks III, C. L., M. Karplus, and B. M. Pettitt. 1988. Proteins: a theoretical perspective of dynamics, structure and thermodynamics. *Adv. Chem. Phys.* 71:1-215.
- Jacrot, B., S. Cusack, and D. M. Engelman. 1982. Inelastic neutron scattering analysis of hexokinase dynamics and its modification on binding to glucose. *Nature (Lond.)*. 300:4-86.
- Middendorf, H. D. 1984. Biophysical applications of quasi-elastic and inelastic neutron scattering. *Annu. Rev. Biophys. Bioeng.* 13:425-451.
- Cusack, S. 1986. Low frequency dynamics of proteins studied by neutron time-of-flight spectroscopy. *Comments Mol. Cell. Biophys.* 3:243-271.
- Smith, J., S. Cusack, U. Pezzeca, B. Brooks, and M. Karplus. 1986. Inelastic neutron scattering analysis of low frequency motion in proteins. *J. Chem. Phys.* 85:3636-3654.
- Cusack, S., J. Smith, J. Finney, B. Tidor, and M. Karplus. 1988. Inelastic neutron scattering analysis of picosecond internal protein dynamics: comparison of harmonic theory with experiment. 202:903-908.
- Altman, P. L., and D. S. Dittmer. 1968. Blood and other body fluids. In *Biology Data Book*. Federation of American Societies for Experimental Biology, Washington DC. 633 pp.
- Smith, J., S. Cusack, P. Poole, and J. Finney. 1987. Direct measurement of hydration-related dynamic changes in lysozyme using inelastic neutron scattering spectroscopy. *J. Biomol. Struct. & Dyn.* 4:583-588.
- Doster, W., S. Cusack, and W. Petry. 1989. Dynamical transition of myoglobin revealed by inelastic neutron scattering. *Nature (Lond.)*. 337:754-756.
- Lovelock, J. E., and M. W. H. Bishop. 1959. Prevention of freezing damage to living cells by dimethyl sulphoxide. *Nature (Lond.)*. 183:1394-1395.
- Brockhouse, B. N. 1961. Inelastic scattering of neutrons in solids and liquids. In *Method for Neutron Spectrometry*. IAEA/Vienna: 113-151.
- Boutin, H., and S. Yip. 1968. Molecular spectroscopy with neutrons. The M.I.T. Press, Cambridge, MA. 74 pp.
- Sears, V. F. 1975. Slow-neutron multiple scattering. In *Advances in Physics*. D. H. Martin, editor. 24:1-45.
- Smith, J., K. Kuczera, B. Tidor, W. Doster, S. Cusack, and M. Karplus. 1989. Direct measurements of hydration related dynamics changes in lysozyme using inelastic neutron scattering spectroscopy. *Physica B*. 156-157:437-443.
- Smith, J., K. Kuczera, and M. Karplus. 1989. Dynamics of myoglobin: comparison of simulation results with neutron scattering spectra. *Proc. Natl. Acad. Sci. USA*. 87:1601-1605.
- Sundaralingam, M., W. Dendel, and M. Greaser. 1985. Stabilization of the long central helix of troponin C by intrahelical salt bridges between amino acid chains. *Proc. Natl. Acad. Sci. USA*. 82:7944-7950.
- Rupley, J. A., P. H. Yang, and G. Tollin. 1980. Water in Polymers, ACS Symposium. S. P. Rowland, editor. American Chemical Society. 127:111-132.
- Poole, P. L., and J. L. Finney. 1983. Hydration induced conformation and flexibility changes in lysozyme at low water content. *Int. J. Biol. Macromol.* 5:308-310.
- Poole, P. L., and J. L. Finney. 1984. Protein hydration and enzyme activity: the role of hydration-induced conformation and dynamic changes in the activity of lysozyme. *Comments Mol. Cell Biophys.* 2:129-151.
- Brooks, C. L., and M. Karplus. 1989. Solvent effects on protein motion and protein effects on solvent motion. *J. Mol. Biol.* 208:159-181.
- Tse, J. S., M. L. Klein, and I. R. McDonald. 1983. Molecular dynamics studies of ice Ic and the structure I clathrate hydrate of methane. *J. Phys. Chem.* 87:4198-4203.
- Dowell, L. G., and A. P. Rinfret. 1960. Low-temperature forms of ice as studied by x-ray diffraction. *Nature (Lond.)*. 188:1144-1148.
- Hartmann, H., F. Parak, W. Steigemann, G. A. Petsko, D. P. Ponzi, and H. Frauenfelder. 1982. Conformational substates in a protein: structure and dynamics of metmyoglobin at 80K. *Proc. Natl. Acad. Sci. USA*. 79:4967-4971.
- Levitt, M., C. Sander, and P. S. Stern. 1985. Protein normal-mode dynamics: trypsin inhibitor, crambin, ribonuclease and lysozyme. *J. Mol. Biol.* 181:423-447.
- Perutz, M. F. 1948. Submicroscopic structure of the red cell. *Nature (Lond.)*. 161:204-205.

- 
29. Painter, P. C., L. E. Mosher, and C. Rhoads. 1982. Low-frequency modes in the Raman spectra of proteins. *Biopolymers*. 21:1469–1472.
30. Brown, K. G., S. S. Erfurth, E. W. Small, and W. L. Peticolas. 1972. Conformationally dependent low-frequency motions of proteins by laser Raman spectroscopy. *Proc. Natl. Acad. Sci. USA*. 69:1467–1469.
31. Elber, R., and W. Karplus. 1986. Multiple conformational states of proteins: a molecular dynamics analysis of myoglobin. *Science (Wash. DC)*. 235:318–321.
32. Wise, W. W., G. C. Wagner, and P. G. Debrunner. 1987. Molecular and electronic reactivity. In *Protein Structure*. R. Austin, E. Buhks, B. Chance, D. DeVault, P. L. Dutton, H. Frauenfelder, and V. I. Goldanskii, editors. Springer, Berlin. 509–510.